Multi-Tag Localization in Cooperative AmBC

Fatemeh Rezaei, *Member, IEEE*, Diluka Galappaththige, *Member, IEEE*, Chintha Tellambura, *Fellow, IEEE,* Amine Maaref, *Senior Member, IEEE*

***Abstract*—We investigate localizing multiple tags in a cooperative ambient backscatter communication (AmBC) network. Firstly, we establish the necessary conditions for the pilots sent by the tags to enable the reader to estimate the directions of arrival (DoAs) of the tags and the radio frequency (RF) source. However, DoA estimation is challenging due to the lower power of tag signals compared to the RF signal. To overcome this, we utilize the Root multiple signal classification (R-MUSIC) and modified subspace methods. These approaches offer significant improvements over the standard MUSIC algorithm. Specifically, we observe an approximate threefold and fivefold enhancement in estimation accuracy, respectively, using only four snapshots of the received signal and a reader with 48 antennas.**

***Index Terms*—Ambient backscatter communication (AmBC), Tag localization, Direction of arrival (DoA) estimation.**

I. Introduction

BACKSCATTER communication (BackCom) networks utilize tags to support Internet of Things (IoT) applications like localization, tracking, and monitoring in domains such as agriculture, manufacturing, logistics, and more [1], [2]. The market value of tags is estimated to be in billions. Determining the positions of tags relative to the reader or transmitter is crucial for these applications. Estimating the direction of arrival (DoA) of tag signals aids in achieving this objective. DoA estimation serves multiple key functions in wireless systems. It helps determine the tags' locations and enables tracking of their movements, if necessary. It also plays a critical role in reducing interference, and mitigating multi-path propagation, thereby enhancing network performance. DoA estimation leads to interference suppression, signal quality improvement, increased reliability, and extended range, and enables precise control of signal directionality through analog beamforming techniques.

This work focuses on DoA estimation for tags in a cooperative ambient backscatter communication (AmBC) setup, encompassing a shared RF source and a reader/receiver serving both primary (cellular) and secondary (backscatter) systems [3], [4]. Tags, functioning as ultra-low-power devices, rely on reflecting RF signals due to limited processing capabilities [1], [5], [6]. The reader, which can be a cell phone user or a Wi-Fi access point, decodes data from both the primary RF source and backscatter tags. As the reader and RF source are integral to the primary networks, a pre-existing connection facilitates the exchange of information, including transmit power and coordinates, via a control link [7]. Consequently, the reader possesses an approximate location of the RF source. Additionally, the reader can estimate the count of dynamically deployed tags through queries, pertinent for applications like tag identification, warehouse monitoring, and localization [8].

Previous DoA estimation studies [9], [10] have mainly focused on single-tag scenarios. For example, to estimate the DoAs of the RF source and the tag, [9] employs the discrete Fourier transformation (DFT) method, and [10] utilizes the multiple signal classification (MUSIC) algorithm. While MUSIC offers higher accuracy than DFT, it requires numerous signal snapshots for satisfactory performance. Notably, neither approach can be extended to estimate the DoAs of multiple tags simultaneously. Moreover, the substantial power differences between the direct-link RF-source signal and the tag signals also limit the localization of tags.

This letter is the first one to develop the DoA estimation of multiple backscatter tags ($K > 1$) – Fig. 1. We assume that the number of active tags (K) is known to the reader, which is a multiple antenna radio. It can estimate the number of active tags via an additional estimation process [8]. Moreover, compressive sensing methods can also estimate the DoAs without knowing the number of tags [11], a promising future research topic. However, we do not treat that estimation problem in order to focus on the DoA estimation problem. In our system, during the estimation phase, all the tags reflect known symbols, i.e., pilots, over the ambient RF source signal. The reader thus receives $K + 1$ signals from the RF source and tags and estimates their DoAs. The main contributions are summarized as follows:

- We propose a novel problem of estimating the DoA of a multi-tag BackCom system. Our study is the first to formulate the problem and develop a solution by defining the necessary conditions for the tag pilots to enable the reader to estimate $K + 1$ different DoAs.
- The tags in the proposed approach use binary phase-shift keying (BPSK) modulation and the Hadamard matrix columns except for the first element as pilots. To evaluate performance, we first utilize the standard MUSIC algorithm with a small number of signal snapshots. As it may not achieve high accuracy due to the significant power level differences between the RF source signal and the tag signals [12], we thus employ the Root-MUSIC (R-MUSIC) algorithm and a modified subspace algorithm.
- The numerical results reveal that the proposed DoA estimation method can achieve reasonable performance even with these standard algorithms. For instance, with 48 reader antennas and 4 received signal snapshots, MUSIC achieves 4.9×10^{-2} root mean square error (RMSE), whereas R-MUSIC and modified subspace algorithms respectively improve the estimation accuracy by 3 and 5 folds, compared to MUSIC.

While classical subspace approaches are commonly used, an alternative modern approach is compressive sensing, which

F. Rezaei, D. Galappaththige, and C. Tellambura are with the Department of Electrical and Computer Engineering, University of Alberta, Edmonton, AB, T6G 1H9, Canada (e-mail: {rezaeidi, diluka.lg, ct4}@ualberta.ca).

A. Maaref is with Huawei Canada, 303 Terry Fox Drive, Suite 400, Ottawa, Ontario K2K 3J1 (e-mail: amine.maaref@huawei.com).

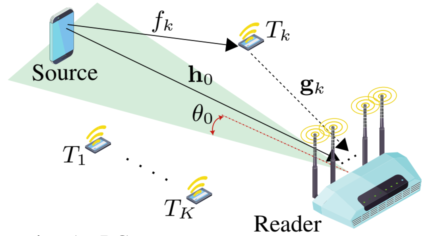

Fig. 1. Cooperative AmBC system setup.

utilizes sparsity and performs well in low signal-to-noise ratio (SNR) conditions [13]. Our study focuses on the multi-tag localization problem, but exploring extensions in this area provides promising opportunities for future research.

Notation: $\mathcal{CN}(\boldsymbol{\mu}, \mathbf{C})$ is a complex Gaussian vector with mean $\boldsymbol{\mu}$ and co-variance matrix $\mathbf{C}$. Denote $\mathcal{K} \triangleq \{1, \ldots, K\}$, $\mathcal{K}_0 \triangleq \{0, 1, \ldots, K\}$, $\mathcal{K}_k \triangleq \mathcal{K}/k$, $\mathcal{N} \triangleq \{1, \ldots, N\}$, and $\mathit{\Theta} \triangleq [-90^\circ : 90^\circ]$.

II. System, Channel, and Signal Models

A. System and Channel Models

We consider a cooperative AmBC system comprising a single-antenna RF source, K single-antenna tags (kth tag is denoted by T_k), and a reader which is equipped with a uniform linear array (ULA) of $M(> K+1)$ antennas (Fig. 1). The system operates on a block flat-fading channel model. During each fading block, $\mathbf{h}_0 = [h_{1,0}, \ldots, h_{M,0}]^{\mathrm{T}} \in \mathbb{C}^{M\times 1}$ is the direct channel response vector from the RF source to the reader. Moreover, $\mathbf{h}_k = f_k \mathbf{g}_k \in \mathbb{C}^{M\times 1}$ for $k \in \mathcal{K}$ is the effective backscatter (cascaded) channel through T_k, which is the product of the forward-link channel from the RF source to T_k, i.e., $f_k \in \mathbb{C}$, and the backscatter channel from T_k to the reader, i.e., $\mathbf{g}_k = [g_{1,k}, \ldots, g_{M,k}]^{\mathrm{T}} \in \mathbb{C}^{M\times 1}$. A unified representation of all channels is given as

$$\mathbf{a}_i = a_i \left[1, e^{j\frac{2\pi d}{\lambda}\sin\theta_i}, \ldots, e^{j\frac{2\pi d}{\lambda}(M-1)\sin\theta_i}\right]^{\mathrm{T}}, \tag{1}$$

where $\mathbf{a}_i \in \{\mathbf{h}_0, \mathbf{g}_k\}$ for $k \in \mathcal{K}$. In (1), λ is the wavelength of the RF signal and d is the distance between the adjacent antennas of the ULA. Besides, $\theta_i \in \mathit{\Theta}$ are the DoAs of incident signals from the tags and the RF source, $a_i \in \{h_0, g_k\}$ denotes the complex gains of the respective channels. Without loss of generality, we assume that the RF source is located around $[-5^\circ : 5^\circ]$ with respect to the reader (Fig. 1).

We make the following key assumptions: (i) the number of tags is known in advance and is upper bounded by the number of antennas at the reader, i.e., $M > K+1$, (ii) all tags reflect during DoA estimation, (iii) and the direct-link channel ($\mathbf{h}_0$) and the cascaded channels ($\mathbf{h}_k$ for $k \in \mathcal{K}$) are mutually uncorrelated.

Since the focus is on passive tags, it is important to describe how energy harvesting (EH) fits into the considered system. Time slots can be partitioned into two distinct phases: (a) denoted as τ, and (b) denoted as τ', illustrated in Fig. 2. During phase (a), the tags just reflect pilot symbols, enabling the reader to execute DoA estimation. In Phase (b), a dual process unfolds: tags transmit their data while simultaneously doing EH by employing power splitting the incoming RF source signal. Both the pilot and data transmission of the tags are facilitated through load modulation. This technique

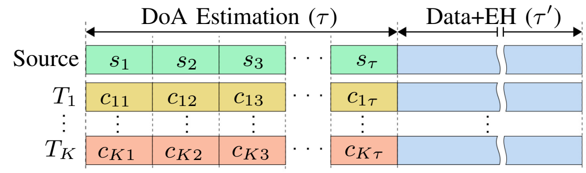

Fig. 2. Transmission framework.

is extremely low power consuming, as elaborated in the references [5], [6]. A concise explanation of load modulation is provided in Section II-B. In our framework, we make the assumption that the energy harvested is substantial enough to effectively support both phases of each tag. Notably, our focus is solely on the development of the DoA estimation aspect. As a result, we omit the intricate details of Phase (b). Nevertheless, it is important to acknowledge that the implications of EH on the tags, the underlying EH models, and other sources of impairment stand as promising avenues for future extensions of this research.

B. Tag's Data/Pilot Transmission

Load modulation involves using a set of load impedances, Z_m's, to generate a multi-level ($\tilde{M}$-ary) signal constellation. To transmit symbol c_m ($\mathbb{E}\{|c_m|^2\} = 1$), the tag presents the impedance Z_m to the antenna of impedance Z_a to generate the reflection coefficient as $\Gamma_m = (Z_m - Z_a^*)/(Z_m + Z_a) = \sqrt{\alpha} c_m$, for $m = \{1, \ldots, \tilde{M}\}$, where $\alpha = |\Gamma_i|^2 \in (0,1]$ is the tag's power reflection factor [5], [6]. For more details on load modulation, see [5], [6] and the references therein.

III. DoA Estimation

We consider the typical frame structure, shown in Fig. 2. The tags backscatter pilot symbols over the RF source signal during the DoA estimation phase of length τ symbols. Let the RF source transmit $\mathbf{s} = [s_1, \ldots, s_\tau]^{\mathrm{T}}$ during period τ, where s_i is the RF source symbol in the ith slot. Without loss of generality, we assume s_i to be a standard circular symmetric complex Gaussian variable, $s_i \sim \mathcal{CN}(0,1)$ [4]. We consider that all K tags transmit pilots during this interval, i.e., T_k backscatters $\mathbf{c}_k = [c_{k1}, \ldots c_{k\tau}] \in \mathbb{C}^{1\times\tau}$, to the reader, where c_{ki} is the transmit tag symbol over s_i. Denoting $\boldsymbol{\beta}_k = [1, e^{j\frac{2\pi d}{\lambda}\sin\theta_k}, \ldots, e^{j\frac{2\pi d}{\lambda}(M-1)\sin\theta_k}]$, we aim to estimate the DoAs, i.e., $\boldsymbol{\beta}_k$ for $k \in \mathcal{K}_0$, of the considered system.

Given the above setup, the received signal at the reader over the i-th RF source symbol, $\mathbf{y}_i \in \mathbb{C}^{M\times 1}$, is given as

$$\mathbf{y}_i = \sqrt{p} h_0 \boldsymbol{\beta}_0 s_i + \sqrt{p} \sum\nolimits_{k\in\mathcal{K}} \sqrt{\alpha_k} h_k \boldsymbol{\beta}_k c_{ki} s_i + \mathbf{n}_i, \tag{2}$$

where $h_k = f_k g_k$, p is the RF transmit power, α_k is T_k's reflection coefficient, and $\mathbf{n}_i \sim \mathcal{CN}(\mathbf{0}, \sigma^2\mathbf{I}_M)$ is the additive white Gaussian noise (AWGN). In (2), we assume that the echoes from the environment and non-tag objects are negligible [9], [10].

Many high-resolution direction-finding methods, including the well-known MUSIC algorithm [14], rely on utilizing the covariance matrix of received signals. The covariance matrix represents the spatial correlation between signals received by different antennas within the array. This information is crucial for determining the DoAs. The initial step involves evaluating the covariance matrix of the received signal over multiple τ RF source symbols. Using (2), it can be obtained as

$$\mathbf{R}_i = \mathbb{E}\left\{\mathbf{y}_i \mathbf{y}_i^{\mathrm{H}}\right\} = p\mathbb{E}\left\{|s_i|^2\right\} \mathbf{Q}_i + \sigma^2 \mathbf{I}, \quad i = 1, \ldots, \tau, \tag{3}$$

where $\mathbf{Q}_i \triangleq (h_0\boldsymbol{\beta}_0 + \sum_{k\in\mathcal{K}}\sqrt{\alpha_k}h_k\boldsymbol{\beta}_k c_{ki})(h_0\boldsymbol{\beta}_0 + \sum_{k\in\mathcal{K}}\sqrt{\alpha_k}h_k\boldsymbol{\beta}_k c_{ki})^{\mathrm{H}} \in \mathbb{C}^{M\times M}$, and $\mathbb{E}\{\mathbf{n}_i\mathbf{n}_i^{\mathrm{H}}\} = \sigma^2\mathbf{I}_M$.

The sum-covariance matrix over τ pilot symbols is $\mathbf{R}_{\mathrm{tot}} = 1/\tau\sum_{i=1}^{\tau}\mathbf{R}_i$. To compute $\mathbf{R}_{\mathrm{tot}}$, we first rewrite $\mathbf{Q}_i$ as

$$\mathbf{Q}_i = \bar{\mathbf{H}}\mathbf{x}_i\mathbf{x}_i^{\mathrm{H}}\bar{\mathbf{H}}^{\mathrm{H}}, \tag{4}$$

where $\bar{\mathbf{H}} \triangleq [h_0\boldsymbol{\beta}_0, \sqrt{\alpha_k}h_k\boldsymbol{\beta}_k, \ldots, \sqrt{\alpha_K}h_K\boldsymbol{\beta}_K] \in \mathbb{C}^{M\times(K+1)}$, and $\mathbf{x}_i = [1, c_{1i}, \ldots, c_{Ki}]^{\mathrm{T}} \in \mathbb{C}^{(K+1)\times 1}$. From (4), $\mathbf{R}_{\mathrm{tot}}$ is thus obtained as

$$\mathbf{R}_{\mathrm{tot}} = p\bar{\mathbf{H}}\mathbf{X}_{\mathrm{tot}}\bar{\mathbf{H}}^{\mathrm{H}} + \sigma^2\mathbf{I}, \tag{5}$$

where $\mathbf{X}_{\mathrm{tot}} \triangleq 1/\tau\sum_{i=1}^{\tau}\mathbf{x}_i\mathbf{x}_i^{\mathrm{H}} \in \mathbb{C}^{(K+1)\times(K+1)}$.

Theorem 1. *$K+1$ different DoAs can be estimated and distinguished from $\mathbf{R}_{\mathrm{tot}}$ (5), if and only if $\mathrm{Rank}(\mathbf{X}_{\mathrm{tot}}) = K+1$ or $\mathrm{Rank}(\mathbf{X}\mathbf{X}^{\mathrm{H}}) = K+1$, where $\mathbf{X} = [\mathbf{x}_1, \ldots, \mathbf{x}_\tau] \in \mathbb{C}^{(K+1)\times\tau}$. Thus, based on eigen-decomposition, $\mathbf{R}_{\mathrm{tot}} = \mathbf{U}\boldsymbol{\Lambda}_t\mathbf{U}^{\mathrm{H}}$, the eigenvector matrix $\mathbf{U}$ is partitioned into a signal matrix $\mathbf{U}_s$ with $K+1$ columns, corresponding to the $K+1$ signal eigenvalues, and a matrix $\mathbf{U}_n$ with $M-(K+1)$ columns, corresponding the noise eigenvalues σ^2.*

Proof. See Appendix A. ■

Following Theorem 1, $\mathbf{X}$ should contain $K+1$ independent rows with all-$\mathbf{1}$ sequence in the first row, and τ must satisfy $\tau \geq K+1$. Otherwise, $K+1$ DoAs cannot be distinguished. One option for $\mathbf{X}$ to satisfy the above design criteria while maintaining the simplicity of tags, is $K+1$ rows of Hadamard matrix of order m, including all-$\mathbf{1}$ sequence, i.e., $\mathbf{H}_m^{\mathrm{h}} \in \{1,-1\}^{m\times m}$, where $m = 2^q$ and $q \geq 1$, satisfying $m \geq K+1$ [15]. Thus, $\tau = m$ and $\mathbf{X}\mathbf{X}^{\mathrm{H}} = \tau\mathbf{I}_{K+1}$. The tags thus adopt BPSK, i.e., $c_{ki} \in \{-1, 1\}$.

Remark 1. *To estimate the DoAs of multiple backscatter tags, the RF source must be treated as an imaginary tag that transmits "1" over different RF source symbols. The tags are then assigned symbols so that the transmitted signals of the tags and the imaginary RF source symbols, i.e., 1's, are mutually orthogonal over τ. Accordingly, Theorem 1 is satisfied, and $K+1$ signal eigenvalues are generated, allowing for successful DoA estimation in BackCom.*

Over the i-th RF source symbol, the tag transmits the ith column of $\mathbf{X}$, excluding the first element. The DoAs are estimated using $\mathbf{R}_{\mathrm{tot}}$ (5) over τ pilot symbols. However, due to the limited signal samples, an estimate of $\mathbf{R}_{\mathrm{tot}}$ is computed as sample covariance $\bar{\mathbf{R}}_{\mathrm{tot}} = 1/(\tau N)\sum_{i=1}^{\tau}\sum_{n=1}^{N}\mathbf{y}_i(n)\mathbf{y}_i^{\mathrm{H}}(n)$, where N is the number of snapshots.

To estimate the DoAs, the conventional MUSIC algorithm can use the sample covariance matrix $\bar{\mathbf{R}}_{\mathrm{tot}}$ by searching for the peaks of the pseudo-spectrum [14]. Specifically, using the orthogonality between arrival angles and noise subspace, the MUSIC pseudo-spectrum is given as

$$P_{\mathrm{MUSIC}} = 1/\|\mathbf{U}_n^{\mathrm{H}}\boldsymbol{\beta}(\theta)\|^2, \tag{6}$$

where $\boldsymbol{\beta}(\theta) = [1, e^{j\frac{2\pi d}{\lambda}\sin\theta}, \ldots, e^{j\frac{2\pi d}{\lambda}(M-1)\sin\theta}]$, for $\theta \in \Theta$. And we search $K+1$ largest peaks of this to estimate DoAs.

As mentioned before, the standard MUSIC algorithm has several drawbacks and cannot resolve the adjacent sources with large power differences [12]. Therefore, we also exploit R-MUSIC and modified subspace algorithms. R-MUSIC, a variant of MUSIC, finds the roots of a polynomial of order $2(M-1)$ [14]. It alleviates the drawbacks of MUSIC and provides improved resolution in low SNR [16]. In contrast, the modified subspace algorithm can resolve weak sources in the vicinity of strong ones and achieve high reliability in low SNRs. Compared to R-MUSIC, the resolution of the modified subspace algorithm improves by increasing the number of antennas. These algorithms are described next.

A. R-MUSIC Algorithm

This method offers advantages in terms of direct calculation of DoA through polynomial zero searches [14]. It reduces computing time and improves angular resolution by leveraging specific properties of received signals.

Let $\mathbf{C} = \mathbf{U}_n\mathbf{U}_n^{\mathrm{H}}$, and the denominator of (6) becomes

$$\begin{aligned}\boldsymbol{\beta}(\theta)^{\mathrm{H}}\mathbf{C}\boldsymbol{\beta}(\theta) &= \sum_{m=0}^{M-1}\sum_{l=0}^{M-1} e^{-j\frac{2\pi d}{\lambda}m\sin\theta}C_{ml}e^{j\frac{2\pi d}{\lambda}l\sin\theta} \\ &= \sum_{\nu=-M+1}^{M-1} c_\nu e^{j\frac{2\pi d}{\lambda}\nu\sin\theta} \\ &\overset{(d)}{=} \sum_{\nu=-M+1}^{M-1} c_\nu z^\nu = D(z),\end{aligned} \tag{7}$$

where $c_\nu = \sum_{n-p=\nu}C_{pn}$, $C_{pn} = [\mathbf{C}]_{(p,n)}$, and (d) is obtained by defining $z = e^{-j\frac{2\pi d}{\lambda}\sin\theta}$.

The roots of $D(z)$ that lie closest to the unit circle correspond to the poles of the MUSIC pseudo-spectrum. These $2(M-1)$ roots can be written as $z_i = |z_i|e^{j\arg(z_i)}$ for $i = \{1, \ldots, 2(M-1)\}$. Hence, choosing those roots inside the unit circle whose magnitude $|z_i| \simeq 1$, and comparing $e^{j\arg(z_i)}$ to $e^{-j\frac{2\pi d}{\lambda}\sin\theta}$ gives

$$\hat{\theta}_i = -\sin^{-1}\left(\lambda\arg(z_i)/2\pi d\right). \tag{8}$$

With perfect covariance measurement, the R-MUSIC polynomial will clearly have $K+1$ roots on the unit circle at the value of z that correspond to the true angles of arrival. However, the noisy measurement causes the roots of the true DoAs to be perturbed away from the unit circle. Hence, from the $2(M-1)$ zeros, R-MUSIC simply chooses the $K+1$ roots with modulus nearest unity among those inside the unit circle.

B. Modified Subspace Algorithm

This exploits the invariance property of noise subspace relative to the source powers [12]. As the source powers change while keeping source directions fixed, the last $M-(K+1)$ eigenvalues/vectors of the covariance matrix remain intact. Accordingly, a virtual source can be introduced whose DoA overlaps with the actual sources, while keeping the noise subspace unchanged. This improves the estimation accuracy and decreases the sensitivity to the power level differences between adjacent sources compared to MUSIC.

Thus, to estimate the DoAs using the modified subspace method, for each value of $\theta \in \Theta$, a new matrix is defined as

$$\mathbf{D}^\theta = \bar{\mathbf{R}}_{\mathrm{tot}} + \eta\boldsymbol{\beta}(\theta)\boldsymbol{\beta}(\theta)^{\mathrm{H}}, \tag{9}$$

where $\eta = \mathrm{Tr}(\bar{\mathbf{R}}_{\mathrm{tot}})/M$. The eigen-decomposition of $\mathbf{D}^\theta$ (9) yields the eigenvalues in the descending order as $\hat{\lambda}_1^\theta \geq \ldots \geq$

TABLE I
ESTIMATED DOAS AND RMSES.

$M=48, \tau=4, N=4, p=20\,\mathrm{dBm}$						
Given Angles (θ)	Estimated			RMSE [Rad]		
	MUSIC	R-MUSIC	Subspace	MUSIC	R-MUSIC	Subspace
$\theta_0 = 5°$	5.0371	5.0045	5.0043	0.0113	0.0038	0.0037
$\theta_1 = -30°$	-29.5228	-29.9697	-29.9828	0.0714	0.0211	0.0139
$\theta_2 = 40°$	39.7078	39.9647	39.9895	0.0473	0.0169	0.0092
$\theta_3 = 15°$	14.8653	14.9820	14.9935	0.0206	0.0076	0.0045

$\hat{\lambda}^{\theta}_{K+1} \geq \ldots \geq \hat{\lambda}^{\theta}_{M}$. The direction of the RF source and tags are those values of θ that correspond to $K+1$ largest peaks of $F(\theta)$ given as [12]

$$F(\theta) = 1 \Big/ \left(\sum\nolimits_{j=K+2}^{M} (\hat{\lambda}^{\theta}_{j} - \bar{\lambda}_j) \right), \tag{10}$$

where $\bar{\lambda}_m$ for $m = \{1, \ldots, M\}$ are the eigenvalues of $\bar{\mathbf{R}}_{\mathrm{tot}}$ that are in decreasing order.

Remark 2. *The computational complexity of the R-MUSIC algorithm is given as $\mathcal{O}(M^3)+\mathcal{O}(M^2(\tau N+K))+\mathcal{O}(M-1)$. Whereas, the computational complexity of the MUSIC algorithm is $\mathcal{O}(M^3)+\mathcal{O}(M^2(\tau N+K+2))+\mathcal{O}((K+1)P)$, where P is the number of scan steps of Θ [16]. Compared to the MUSIC algorithm, the modified subspace algorithm requires the eigendecomposition of a $M \times M$-dimensional matrix for each value of $\theta \in \Theta$, with the complexity $\mathcal{O}((P+1)M^3) + \mathcal{O}(M^2(\tau N+P+1)) + \mathcal{O}((K+1)P)$.*

Remark 3. *Although we focus on cooperative AmBC, our method can also work for other BackCom configurations, i.e., monostatic and bistatic. Specifically, for monostatic BackCom, with co-located RF source and reader, the direct-link signal, the first term in* (2)*, disappears. However, to estimate DoAs, the correlation between the tag-to-reader and reader-to-tag channels must be considered.*

TABLE II
SIMULATION SETTINGS.

Parameter	Value	Parameter	Value
τ	4	M	48
K	3	α	0.8, 0.6
N	1,4	σ^2	1

IV. SIMULATION RESULTS

We give simulations to validate the proposed estimators. We consider $K = 3$ tags with the DoAs $[\theta_1, \theta_2, \theta_3] = [-30°, 40°, 15°]$, and $\theta_0 = 5°$. All channels are modeled as $f_k, g_k, h_0 \sim \mathcal{CN}(0,1)$, and $\sigma^2 = 1$. We set $\tau = 4$, $d = \lambda/2$, $\alpha_k = 0.8, \forall k$. As a benchmark, we also consider MUSIC.

We assess the quality of the DoA estimator in terms of RMSE, which is defined as

$$\mathrm{RMSE}\,[\mathrm{Rad}] = \sqrt{\frac{1}{\mathcal{I}(K+1)} \sum\nolimits_{k \in \mathcal{K}_0} (\theta_k - \hat{\theta}_k)^2}, \tag{11}$$

where $\mathcal{I}$ denotes the number of Monte Carlo trials.

Fig. 3 depicts the RMSEs achieved by different methods versus the transmit power for $M = 48$ antennas at the reader. The individual RMSEs are also given in Table I. As observed, the R-MUSIC and modified subspace methods improve the DoA estimation and significantly outperform the MUSIC algorithm with only a few snapshots. In particular, at $19\,\mathrm{dBm}$ transmit power of the RF source and $N = 4$, the RMSEs achieved by MUSIC, R-MUSIC, and modified subspace are respectively 0.049, 0.016, and 0.01. Additionally, the modified subspace method provides higher accuracy than R-MUSIC, especially for a higher number of snapshots.

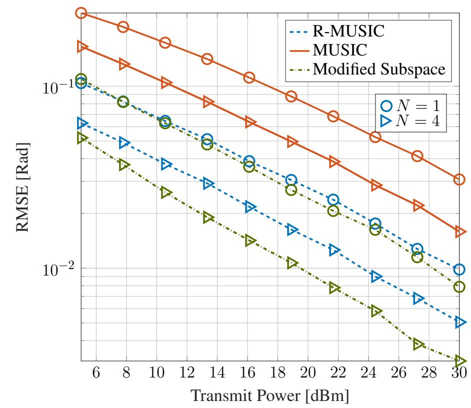

Fig. 3. RMSE versus transmit power for $M = 48$, $\alpha = 0.8$, and different number of snapshots, $N = \{1, 4\}$.

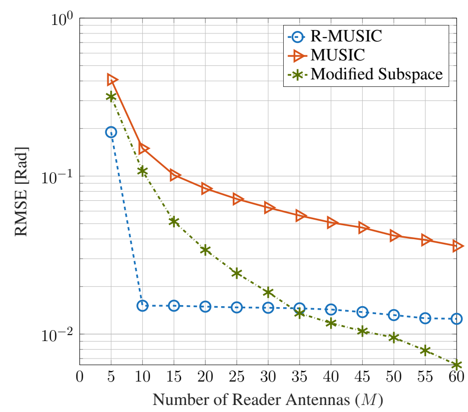

Fig. 4. RMSE versus reader antennas M, for $p = 20\,\mathrm{dBm}$, $\alpha = 0.8$, and $N = 4$.

Fig. 4 investigates the effect of the number of reader's antennas on the DoA estimation accuracy, for $p = 20\,\mathrm{dBm}$, and $N = 4$. As expected, when the reader has more antennas, the RMSEs decrease as the reader's ability to distinguish spatial signals is enhanced. While the R-MUSIC algorithm has a higher angular resolution for a lower number of antennas at the reader, its accuracy slightly improves with increased antennas when compared to MUSIC and subspace algorithms.

We also investigate the effect of the number of snapshots, N, on the DoA estimation in Fig. 5, for $p = 20\,\mathrm{dBm}$ and $M = 32$. Increasing the number of snapshots significantly improves the performance of the modified subspace method, compared to the others. Specifically, when the number of snapshots is increased from 4 to 12, the accuracy of the modified subspace method increases by $102\,\%$, while $62\,\%$ and $34\,\%$ improvements are achieved for MUSIC and R-MUSIC

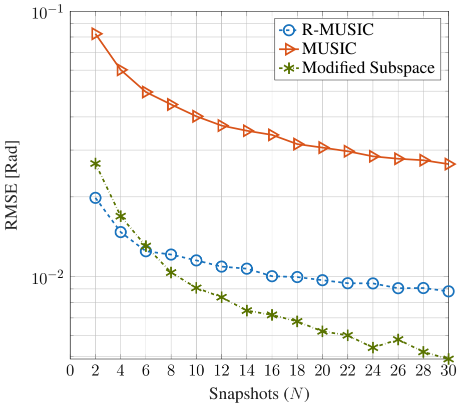

Fig. 5. RMSE versus number of snapshots N, for $p = 20\,\mathrm{dBm}$, $\alpha = 0.8$, and $M = 32$.

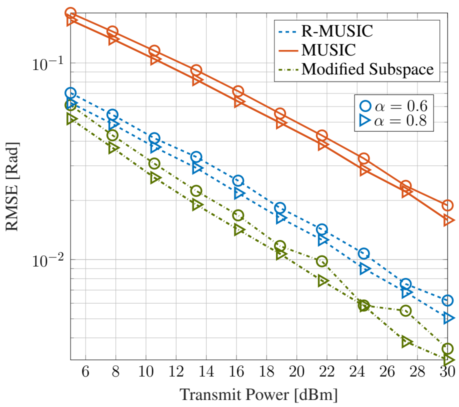

Fig. 6. RMSE versus transmit power, for $N = 4$, $M = 48$, and different reflection coefficient at the tags, $\alpha = \{0.6, 0.8\}$.

algorithms. The above simulations reveal that the modified subspace method achieves highly accurate DoA estimates, using a large number of antennas at the reader, and a few snapshots of the received signal.

Finally, Fig. 6 plots the RMSE for $\alpha = \{0.6, 0.8\}$ to examine the impact of reflected power by the tags on the quality of the DoA estimation. Higher α increases the reflected power at each tag, improving the estimation quality.

V. Conclusion

We investigated the problem of DoA estimations for multiple tags in a cooperative AmBC network. We designed a frame structure for the pilot signals reflected by the tags. By doing so, we derived a set of essential conditions for these pilot signals that facilitate the reader's ability to discern the DoAs of both the tag signals and the RF source signal. Subsequently, we employed the R-MUSIC and modified subspace methods for the DoA estimation process. To elaborate, even with a limited array of 48 antennas at the reader and a modest number of signal snapshots, the modified subspace method provides high accuracy. Notably, the R-MUSIC algorithm performs better when the number of antennas at the reader is small.

Our work is the first one to study this problem for multiple tags. As such, it paves the way for several future directions, including exploring i) non-uniform antenna arrays at the reader, ii) under-determined cases with more signal sources than reader antennas, and iii) scenarios with an unknown number of tags. Estimators based on compressive sensing and neural networks should also be investigated.

Appendix A: Proof of Theorem 1

Since $\mathrm{Rank}(\bar{\mathbf{H}}) = K+1$, with Schmidt orthogonalization, we can obtain $K+1$ normalized orthogonal vectors from $\bar{\mathbf{H}}$, i.e., $[\mathbf{v}_0, \ldots, \mathbf{v}_K]$, which satisfies $[\mathbf{v}_0, \ldots, \mathbf{v}_K]\bar{\mathbf{V}} = \bar{\mathbf{H}}$, where $\bar{\mathbf{V}} = [\bar{\mathbf{v}}_0, \bar{\mathbf{v}}_1, \ldots, \bar{\mathbf{v}}_K] \in \mathbb{C}^{(K+1)\times(K+1)}$, with the kth column, $k \in \mathcal{K}_0$, $\bar{\mathbf{v}}_k = [\eta_{k0}, \eta_{k1}, \ldots, \eta_{k(k-1)}, \eta_{kk}, 0, 0, \ldots, 0]^{\mathrm{T}}$, in which $\eta_{kj} = \|\bar{h}_k\boldsymbol{\beta}_k - \sum_{j=0}^{k-1}\eta_{kj}\frac{\bar{h}_j\boldsymbol{\beta}_j}{\|\bar{h}_j\boldsymbol{\beta}_j\|}\|; k = j$, and $\frac{\bar{h}_j^*\bar{h}_k\boldsymbol{\beta}_j^{\mathrm{H}}\boldsymbol{\beta}_k}{\|\bar{h}_j\boldsymbol{\beta}_j\|}; 0 \leq j < k$, where $\bar{h}_k = \sqrt{\alpha_k}h_k, k \in \mathcal{K}$. Therefore, (5) can be written as $\mathbf{R}_{\mathrm{tot}} = \mathbf{R}_s + \sigma^2\mathbf{I}$, where $\mathbf{R}_s = [\mathbf{v}_0, \ldots, \mathbf{v}_K]\mathbf{U}\Lambda\mathbf{U}^{\mathrm{H}}[\mathbf{v}_0, \ldots, \mathbf{v}_K]^{\mathrm{H}}$, and $\bar{\mathbf{V}}\mathbf{X}_{\mathrm{tot}}\bar{\mathbf{V}}^{\mathrm{H}} = \mathbf{U}\Lambda\mathbf{U}^{\mathrm{H}}$, using eigen-decomposition. Thus, in order that $\mathrm{span}(\boldsymbol{\beta}_0, \ldots, \boldsymbol{\beta}_K) = \mathrm{span}([\mathbf{v}_0, \ldots, \mathbf{v}_K]\mathbf{U})$, we should have $\mathrm{Rank}(\bar{\mathbf{V}}\mathbf{X}_{\mathrm{tot}}\bar{\mathbf{V}}^{\mathrm{H}}) = K+1$, i.e., $\mathrm{Rank}(\mathbf{X}_{\mathrm{tot}}) = K+1$. Besides, $\forall\mathbf{u}_m \in \mathbf{U}$, $\mathbf{R}_s\mathbf{u}_m = \lambda_m\mathbf{u}_m$, we have $\mathbf{R}_{\mathrm{tot}}\mathbf{u}_m = \mathbf{R}_s\mathbf{u}_m + \sigma^2\mathbf{I}\mathbf{u}_m = (\lambda_m + \sigma^2)\mathbf{u}_m$, i.e., any eigenvector of $\mathbf{R}_s$ is also an eigenvector of $\mathbf{R}_{\mathrm{tot}}$ with corresponding eigenvalue $(\lambda_m + \sigma^2)$. Thus, $\mathbf{R}_{\mathrm{tot}} = \mathbf{U}\boldsymbol{\Lambda}_t\mathbf{U}^{\mathrm{H}}$, where $\boldsymbol{\Lambda}_t = (\boldsymbol{\Lambda} + \sigma^2\mathbf{I})$, i.e, $\boldsymbol{\Lambda}_t = \mathrm{diag}(\lambda_0 + \sigma^2, \lambda_1 + \sigma^2, \ldots, \lambda_K + \sigma^2, \sigma^2, \ldots, \sigma^2)$, corresponding to the signal and noise subspaces.

References

[1] H. Huawei, "3GPP TSG Meeting −97e, New SID: S: Study on Ambient IoT, (from RP-222685)," Sep. 2022. Available Online: https://portal.3gpp.org/ngppapp/TdocList.aspx?meetingId=60289.

[2] "3GPP TSG RAN −94e, Moderator's summary for discussion [RAN94e-R18Prep-28] passive IoT (from RP-212688)," Dec. 2021. Available Online: https://portal.3gpp.org/ngppapp/TdocList.aspx?meetingId=60043.

[3] G. Yang, Q. Zhang, and Y.-C. Liang, "Cooperative ambient backscatter communications for green internet-of-things," *IEEE Internet Things J.*, vol. 5, no. 2, pp. 1116–1130, Apr. 2018.

[4] R. Long, Y.-C. Liang, H. Guo, G. Yang, and R. Zhang, "Symbiotic radio: A new communication paradigm for passive internet of things," *IEEE Internet Things J.*, vol. 7, no. 2, pp. 1350–1363, 2020.

[5] F. Rezaei, D. Galappaththige, C. Tellambura, and S. Herath, "Coding techniques for backscatter communications - A contemporary survey," *IEEE Commun. Surveys Tuts.*, pp. 1020–1058, 2th Quart. 2023.

[6] D. Galappaththige, F. Rezaei, C. Tellambura, and S. Herath, "Link budget analysis for backscatter-based passive IoT," *IEEE Access*, vol. 10, pp. 128 890–128 922, Dec. 2022.

[7] "Positioning techniques for mobile devices in LTE," July 2015. Available Online: https://www.hsc.com/resources/blog/positioning-techniques-for-mobile-devices-in-lte/.

[8] M. Shahzad and A. X. Liu, "Fast and accurate estimation of RFID tags," *IEEE/ACM Trans. Networking*, vol. 23, no. 1, pp. 241–254, Jan. 2014.

[9] W. Zhao, G. Wang, S. Atapattu, R. He, and Y.-C. Liang, "Channel estimation for ambient backscatter communication systems with massive-antenna reader," *IEEE Trans. Veh. Technol.*, vol. 68, no. 8, pp. 8254–8258, Aug. 2019.

[10] S. Li, J. Ge, and Y.-C. Liang, "Azimuth estimation for the backscatter device in ambient backscatter communication system," *IEEE Wireless Commun. Lett.*, vol. 11, no. 8, pp. 1674–1678, Aug. 2022.

[11] M. Dehghani and K. Aghababaiyan, "FOMP algorithm for direction of arrival estimation," *Physical Commun.*, vol. 26, pp. 170–174, Feb. 2018.

[12] A. Olfat and S. Nader-Esfahani, "A new signal subspace processing for DOA estimation," *Signal Process.*, vol. 84, no. 4, pp. 721–728, Apr. 2004.

[13] K. Aghababaiyan, V. Shah-Mansouri, and B. Maham, "High-precision OMP-based direction of arrival estimation scheme for hybrid non-uniform array," *IEEE Commun. Lett.*, vol. 24, no. 2, pp. 354–357, Feb. 2020.

[14] A. Swindlehurst and T. Kailath, "A performance analysis of subspace-based methods in the presence of model errors. I. the MUSIC algorithm," *IEEE Trans. Signal Process.*, vol. 40, no. 7, pp. 1758–1774, July 1992.

[15] K. J. Horadam, *Hadamard matrices and their applications*. Princeton university press, Jan. 2012.

[16] E. Gentilho Jr, P. R. Scalassara, and T. Abrão, "Direction-of-arrival estimation methods: A performance-complexity tradeoff perspective," *J. Signal Process. Syst.*, vol. 92, no. 2, pp. 239–256, Feb. 2020.